

Effective Hamiltonian Study on the Valence States of NH and NH⁺

Jong Keun Park and Hosung Sun *

Department of Chemistry, Pusan National University, Pusan 609-735. Received October 25, 1989

The second order *ab initio* effective valence shell Hamiltonian is calculated for the valence state potential energy curves of NH and NH⁺. From the potential energy curves various spectroscopic constants of valence states are determined. The results are in good agreement with experiments and configuration interaction calculations. They show the composite picture of potential energy curves and also indicate that the second order effective Hamiltonian theory is adequate for describing various valence states of a molecule and its ions simultaneously.

Introduction

The *ab initio* effective valence shell Hamiltonian (H^p) which is based on quasidegenerate many-body perturbation theory (QDMBPT) has been applied to various atomic and molecular systems¹⁻²¹. From these applications it is understood that the H^p method is exact in principle and accurate for theoretically calculating electronic structures of molecules. The advantage in using H^p is that i) H^p produces all valence state energies with a same accuracy and ii) H^p simultaneously describes a molecule and its ions, and thus saves a lot of computer CPU time.

The main purpose of this work is to understand the behavior of effective valence shell Hamiltonian more deeply. The quasidegenerate many-body perturbation theory on which the H^p method is based is relatively new method for studying various electronic states of molecules on an equal footing. The similar multi-reference MBPT has been recently developed, but not many applications have been reported yet^{22,23}. The H^p is a pioneer of multi-reference MBPT, though the theory itself is called QDMBPT instead of multi-reference MBPT. Therefore the deeper understanding on H^p is very helpful for developing more reliable *ab initio* theory of electronic structures. Furthermore the H^p formally mimics semiempirical theories of valence. So the H^p study greatly enhances the development of semiempirical theories²⁴⁻²⁶.

In the present work we apply the second order H^p to various geometries of NH and NH⁺. The astrophysically important NH species have been studied experimentally²⁷⁻³⁶ and theoretically³⁷⁻⁵⁵ before. Nevertheless only low-lying states have been investigated so far. In particular for NH⁺ ion, only doublet states have been theoretically studied. Given the effort to determine the potential curve for one valence state, all the other valence state potential curves for neutral NH and its ions are easily generated by the H^p approach with virtually no additional labor. This is one of the advantages of the H^p treatment. In addition, one H^p calculation also yields higher-lying valence state potential curves which are determined simultaneously with the low-lying states and which should have a similar accuracy. Therefore we virtually investigate all the valence states of NH and NH⁺. This extensive study first reveals that the first excited state of NH⁺, i.e., ⁴ Σ^- state does actually crosses the ground state, ² Π .

In the following theory section the characteristics and properties of H^p formalism is briefly summarized. In the calculations section, the detailed computational procedure, e.g., the basis set, self-consistent-field(SCF) procedure, the choi-

ce of orbital energies, evaluation of H^p matrix elements, and diagonalization of valence CI matrix, are discussed. Results and discussion are provided in the last section.

Theory

In perturbation treatment the molecular electronic Hamiltonian H can be decomposed into a zeroth order part H_0 and a perturbation V ,

$$H = H_0 + V \quad (1)$$

When H_0 is constructed as a sum of one-electron Fock operators, then the perturbation V contains what we call the correlation corrections. The full many-electron Hilbert space can be divided into primary space with projector P_0 and its orthogonal complement with projector $Q_0 = 1 - P_0$. The P_0 space is supposedly taken to contain a set of many electron basis functions which are quasidegenerate with respect to the zeroth order Hamiltonian H_0 . Our choice below for P_0 takes it to span the valence space of all distinct configuration state functions involving a filled core and the remaining electrons distributed among the valence orbitals. Hence, the Q_0 space contains all basis functions with at least one core hole and/or one occupied excited orbital.

Quasidegenerate many-body perturbation theory transforms the full Schrödinger equation

$$H\Psi_i = E\Psi_i \quad (2)$$

into the P_0 space effective valence shell Schrödinger equation

$$H^p\Psi_i^v = E\Psi_i^v \quad (3)$$

for the projection $\Psi_i^v = P_0\Psi_i$, where the E are the exact eigenvalues of equation (2). Then, quasidegenerate perturbation theory gives the second order approximation

$$H^p = P_0 H P_0 + \frac{1}{2} \sum_{\Lambda, \Lambda'} (P_0(\Lambda) V Q_0 (E_\Lambda - H_0)^{-1} V P_0(\Lambda') + h.c.) \quad (4)$$

where *h.c.* designates the Hermitian conjugate of the preceding term and $P_0(\Lambda)$ designates the projector onto the valence space basis function $|\Lambda\rangle$. Here H^p is called the effective valence shell Hamiltonian.

The equation (4) can be expanded within the orbital basis set. This tedious algebraic procedure requires so called

diagrammatic expansion technique, and the explicit formula can be found elsewhere⁸. We can group the expansion terms into several categories and the grouped terms are usually classified as E_c (core energy), H_i^v (one-electron term), H_{ij}^v (two-electron term), and H_{ijk}^v (three-electron term). The expectation values of the effective operators (E_c , H_i^v , etc.) are called matrix elements of H^v . (They are called parameters in semiempirical theories). And these matrix elements should be numerically computed to determine valence state energies. Therefore we formally rewrite the H^v expression as

$$H^v = E_c + \sum_i H_i^v + \frac{1}{2} \sum_{i,j} H_{ij}^v + \frac{1}{3!} \sum_{i,j,k} H_{ijk}^v + \dots \quad (5)$$

The effective valence shell Hamiltonian, H^v has the following properties:

(1) H^v contains reference to only some prechosen set of valence shell orbitals. H^v depends explicitly on which orbitals are chosen for the valence shell. Nevertheless the eigenvalues of H^v are exactly identical to the corresponding valence shell energies (*i.e.*, potential energy surfaces) which result from the full molecular Schrödinger equation for the valence states.

(2) The exact eigenvalues of H^v are obtained from a complete valence shell configuration interaction calculation. Hence, H^v is the quantity which is mimicked by semiempirical model Hamiltonians where the parameterization-configuration interaction paradox is removed by this definition of H^v .

(3) H^v can be shown to have matrix elements between N_v -electron Slater determinants of valence shell orbitals which differ by 0, 1, 2, 3, 4, ..., N_v spin-orbitals. The 3, 4, ..., N_v cases imply that H^v must contain operator, H_{ijk}^v , H_{ijkl}^v , ..., which explicitly act on the coordinates of 3, 4, ..., N_v -electrons. These are many-electron operators, which have no counterparts in traditional semiempirical theories. With hindsight, this result should not be terribly surprising, in view of the fact that H^v must produce exact energies with only a "minimum" basis set of valence orbitals. Hence, part of the work, done by the remaining (infinite) set of complete basis orbitals in normal *ab initio* calculations, is accomplished by these many-electron operators in the effective Hamiltonian theory in order to make H^v give exact energies.

(4) H^v uses the same valence orbitals for all valence states of the system (including all different charge states!). This differs markedly from the procedure in *ab initio* calculations where the nature of the orbitals varies with the state and charge (*e.g.*, ions *vs.* neutrals). Despite this enormous difference, H^v may be used for all these valence states because it is exact.

(5) The actual evaluation of the individual matrix elements of H_i^v , H_{ij}^v , H_{ijk}^v , ... in the valence shell basis set requires somewhat more work than the direct calculation of the state energies by equivalent configuration interaction calculation of the state energies by equivalent configuration interaction calculations, because we require additional information, *viz.*, the individual matrix elements of H_i^v , H_{ij}^v , H_{ijk}^v , However, the net bonus is the fact that an H^v calculated for a neutral system can also be used for its ion (positive and negative). In fact, the ion calculations are then simple to carry out as in semiempirical theories.

Calculations

Table 1. Contracted Gaussian Basis Set (Ref. 56)

type	N		H	
	exponent	contraction coefficient	exponent	contraction coefficient
s	5909.4400	0.002004	19.2406	0.032828
s	887.4510	0.015310	2.8992	0.231208
s	204.7490	0.074293	0.6534	0.817238
s	59.8376	0.253364		
s	19.9981	0.600576		
s	2.6860	0.245111		
s	7.1927	1.000000	0.1776	1.000000
s	0.7000	1.000000		
s	0.2133	1.000000		
p	26.7860	0.038244	1.08 ^a	1.000000
p	5.9564	0.243846		
p	1.7074	0.817193		
p	0.5314	1.000000		
p	0.1654	1.000000		
d	0.67 ^a	1.000000		

^aRef. 57.

A basis set which consists of basis functions is chosen as a set of contracted Gaussian functions. These are composed of the Dunning's 4s3p contracted Gaussians from 9s5p primitive Gaussians for nitrogen and 2s from 4s primitive Gaussians for hydrogen⁵⁶. To include electron correlations properly in a later stage of H^v calculation, a polarization function, *d* is added to the nitrogen basis and a *p* polarization function is added to the hydrogen basis⁵⁷. This kind of basis set is called the double zeta plus polarization basis and its usefulness has been well tested before⁵⁷. This basis set is listed in Table 1.

In the previous H^v calculations it has been verified that the second order H^v contains most of electron correlations. So in the present work we adopt the second order H^v formalism. In H^v calculations the valence space has to be predetermined. The valence space consists of configuration state functions arising from 2σ, 3σ, 1π_x, 1π_y, and 4σ orbitals. This choice is appropriate because these molecular orbitals come from valence orbitals of N(2s and 2p) and H(1s). 1σ orbital is considered as a core orbital and its electronic configuration is fixed as filled, *i.e.*, 1σ² all the way. However, one should note that the H^v naturally includes all of core-core, core-valence and core-excited correlations. 5σ and higher-lying orbitals are classified as excited orbitals.

The zeroth order Hamiltonian chosen in H^v formalism is a diagonal one-electron operator. The diagonal elements of zeroth order Hamiltonian are called orbital energies. In principle the choice of orbital energies is quite arbitrary (this is a good advantage of H^v method), though a bad choice may slow down the convergence of the perturbation expansion of H^v . In the present work, to determine diagonal elements of H_0 , first the SCF calculations were performed to have a reasonable set of molecular orbitals. For NH, the SCF was performed for the ground ³Σ⁻ state. Since H^v describes all valence states on an equal footing, only one SCF calculation is necessary enough for producing all other valence states. The same set of molecular orbitals are used for both of NH and NH⁺. Orbital energies for NH states are taken from the

diagonal elements of Fock operator of the ground $^3\Sigma^-$ state of neutral NH. For NH^+ calculations a new Fock diagonal elements which best describes the $^1\Sigma^+$ state of NH^{+6} are constructed. These diagonal elements have much lower energies than those from neutral NH. This set of orbital energies are called bare core orbital energies. This choice is found to best reproduce the ionic NH^+ valence states. To guarantee the fast convergence of the second order H^p , orbital energies for valence orbitals (2σ , 3σ , $1\pi_x$, $1\pi_y$, and 4σ) are arithmetically averaged.

The H^p matrix elements are composed of the core energy (E_c), one-electron, two-electron, and three-electron matrix elements. The core energy is the energy of $1\sigma^2$ configuration including all the core-core, core-valence, and core-excited correlations. The one-electron H_i^p matrix elements are denoted as $\langle 2\sigma | H_i^p | 2\sigma \rangle$, etc. Two-electron H_{ij}^p matrix elements are as $\langle 2\sigma 2\sigma | H_{ij}^p | 2\sigma 2\sigma \rangle$, etc. Here $\langle 2\sigma 2\sigma | H_{ij}^p | 2\sigma 2\sigma \rangle$ means $\iint 2\sigma(1)2\sigma(2) | H_{ij}^p | 2\sigma(1)2\sigma(2) d\tau_1 d\tau_2$. Three-electron ones are as $\langle 3\sigma 2\sigma 2\sigma | H_{ijk}^p | 3\sigma 2\sigma 2\sigma \rangle$ etc. The three electron H^p matrix elements should exist because the H^p is the effective Hamiltonian, which means that the whole H operator is projected the small valence space, P_v . In the second order H^p expression, the four- or higher-electron terms do not appear. These matrix elements of H^p are computed within the second order expansion.

With these H^p matrix elements, we can set up the small valence configuration interaction(CI) matrix. The valence CI matrix consists of integral values of various valence configuration state functions with H^p operator. After diagonalizing the valence CI matrix, we can obtain the valence state energies. This valence CI matrix is, of course, very small compared with the usual full CI matrix. And all the valence state energies resulting from the valence CI matrix are calculated with a same accuracy. Naturally all the electron correlations are also included. The valence state energies are electronic energies under the Born-Oppenheimer approximation and, next, the nuclear repulsion energy is added to them in order to obtain the total energies of valence states.

The whole procedure has been repeated by changing internuclear distance (R) between N and H . The internuclear distances where H^p calculations were performed are 1.3, 1.5, 1.7, 1.9, 1.958, 2.0, 2.2, 2.4, 2.6, 2.8, 3.0, 3.2, 3.4, 3.5, 4.0, 4.5, and 5.0 au. When R is larger than 5.0 au, the configuration mixing gets to be strong. So SCF procedure is not appropriate to determine molecular orbitals. Therefore, in the present work, H^p calculations at large R are not performed. Instead H^p calculations for atomic N and H are separately performed to determine separate atom limits correctly. And potential curves are interpolated between $R = 5.0$ au and separate atom limits.

Spectroscopic constants for several low-lying states of NH and NH^+ were determined by fitting the calculated potential energy curves to an eighth degree polynomial. From this, Dunham coefficients are computed to obtain R_e , ω_e , $\omega_e x_e$, B_e , α_e , and D_e values.

Results and Discussion

The calculated SCF energy for the $X^3\Sigma^-$ state of NH at $R = 1.985$ au is -54.96795 au. Meyer and Rosmus⁵¹ used a large Gaussian basis set ($4s4p2d1f/4s2p1d$) and their energy was -54.977 au. Bauschlicher and Langhoff's⁵⁰ value was -55.000417 au at $R = 1.963$ au and they adopted a huge basis set, $5s4p3d2f1g/4s3p2d$. Our basis $4s3p1d/2s1p$ is smaller than that in either of the two calculations. So our SCF energy is expected to be higher than those. But it turns out that our value is not so much higher than them, which shows our basis set is reasonably good enough.

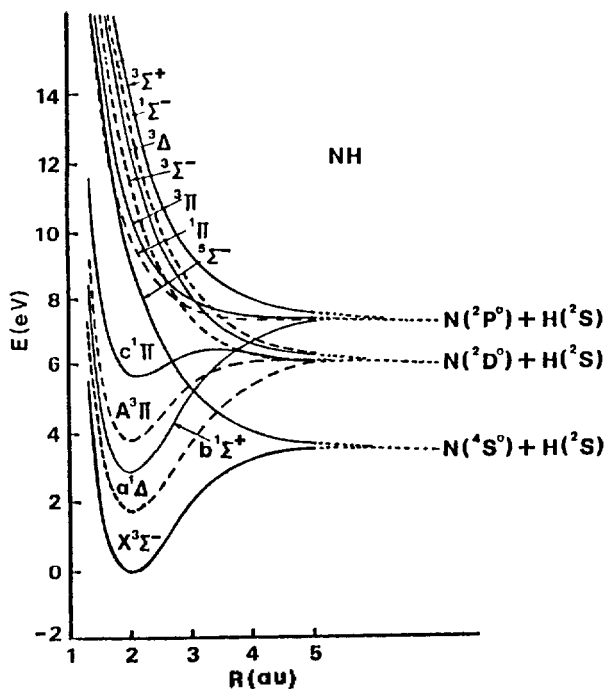
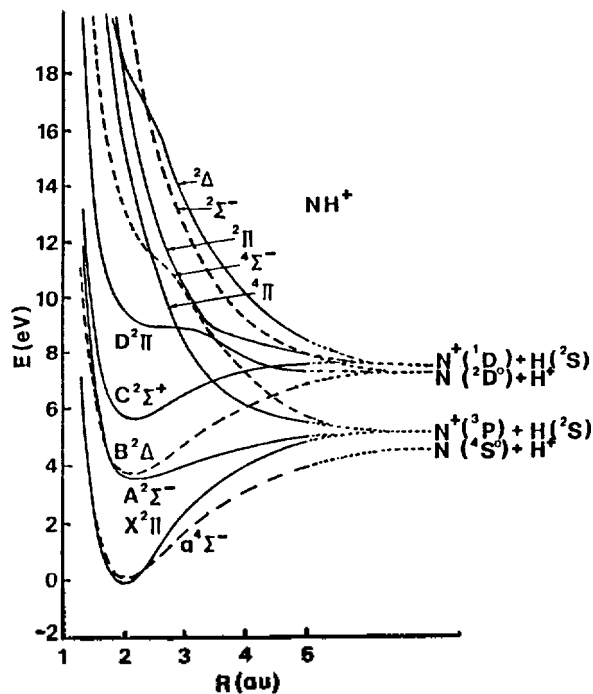
In H^p calculations the core energy(E_c) is negative, one-electron matrix elements (H_i^p) are generally negative, but two-electron matrix elements (H_{ij}^p) are positive as expected. The three electron matrix elements (H_{ijk}^p) which do not exist in ordinary semiempirical theories are usually small. However, the ignorance of those three-electron matrix elements give erroneous results in the valence state energies. It implies that, in semiempirical theories, the contribution

Table 2. Second Order H^p Total Energies (au) of NH as a Function of Internuclear Distance (au)

R	$X^3\Sigma^-$	$a^1\Delta$	$b^1\Sigma^+$	$A^3\Pi$	$c^1\Pi$	$^5\Sigma^-$
1.3	-54.944908	-54.877396	-54.833524	-54.804009	-54.712803	-54.457556
1.5	-55.076241	-55.009369	-54.965367	-54.933331	-54.847819	-54.612911
1.7	-55.135083	-55.068320	-55.024114	-54.990371	-54.911097	-54.707702
1.9	-55.155035	-55.087903	-55.043598	-55.008474	-54.936117	-54.773321
1.958	-55.156426	-55.089535	-55.044788	-55.009401	-54.939186	-54.789350
2.0	-55.156539	-55.089597	-55.044739	-55.009213	-54.940589	-54.800336
2.2	-55.149598	-55.082261	-55.036850	-55.001616	-54.941005	-54.840804
2.4	-55.135126	-55.067105	-55.021101	-54.987752	-54.935769	-54.884984
2.6	-55.117553	-55.048508	-55.001889	-54.972186	-54.929161	-54.915886
2.8	-55.099685	-55.029245	-54.982019	-54.957863	-54.923664	-54.940571
3.0	-55.082710	-55.010493	-54.962677	-54.946127	-54.920025	-54.959629
3.2	-55.067899	-54.993483	-54.945216	-54.937843	-54.918528	-54.974472
3.4	-55.055579	-54.978583	-54.929962	-54.932743	-54.918645	-54.985882
3.5	-55.050391	-54.971995	-54.923203	-54.931135	-54.919092	-54.990542
4.0	-55.033539	-54.947727	-54.898152	-54.930673	-54.923061	-55.006818
4.5	-55.027335	-54.933140	-54.883107	-54.930074	-54.924138	-55.013943
5.0	-55.027177	-54.936008	-54.882084	-54.929874	-54.925674	-55.017388
∞	-55.026456	-54.929545	-54.880588	-54.929545	-54.929545	-55.026453

Table 3. Second Order H^p Total Energies (au) of NH⁺ as a Function of Internuclear Distance (au)

R	$X^2\Pi$	$a^4\Sigma^-$	$A^2\Sigma^-$	$B^2\Delta$	$C^2\Sigma^+$	$^4\Pi$
1.3	-54.444583	-54.445477	-54.294294	-54.320296	-54.252473	-53.770529
1.5	-54.583999	-54.582555	-54.440629	-54.460240	-54.393136	-53.954165
1.7	-54.647310	-54.645157	-54.513234	-54.526096	-54.459981	-54.066877
1.9	-54.668754	-54.667190	-54.551623	-54.548999	-54.486627	-54.145340
1.958	-54.670099	-54.669033	-54.552605	-54.554540	-54.489901	-54.165160
2.0	-54.670105	-54.669488	-54.553285	-54.555774	-54.491414	-54.179024
2.2	-54.662323	-54.664707	-54.558952	-54.554776	-54.491787	-54.240312
2.4	-54.647282	-54.653674	-54.557809	-54.547439	-54.485893	-54.293632
2.6	-54.629860	-54.640702	-54.553845	-54.537903	-54.477851	-54.338490
2.8	-54.613141	-54.628232	-54.549343	-54.528453	-54.470004	-54.376281
3.0	-54.598404	-54.620668	-54.545324	-54.519824	-54.463233	-54.408148
3.2	-54.585218	-54.606815	-54.541569	-54.511702	-54.457359	-54.433390
3.4	-54.573382	-54.597381	-53.537883	-54.504040	-54.452439	-54.452495
3.5	-54.567898	-54.592981	-54.536077	-54.500399	-54.450368	-54.460117
4.0	-54.544764	-54.574256	-54.528047	-54.484303	-54.443802	-54.485051
4.5	-54.529431	-54.560385	-54.521899	-54.471546	-54.442504	-54.497693
5.0	-54.519923	-54.549957	-54.517128	-54.461295	-54.443084	-54.497693
∞	-54.509765	-54.526456	-54.509765	-54.429545	-54.427655	-54.503822

**Figure 1.** Potential energy curves for NH from the second order H^p calculation.**Figure 2.** Potential energy curves for NH⁺ from the second order H^p calculation.

from three-electron terms is somehow embedded into one- and two-electron parameters. Of course the diagonal H^p matrix elements are larger than the off-diagonal elements.

At $R = 1.985$ au, the total energy of $X^3\Sigma^-$ of NH is -55.15654 au. The difference between the SCF energy and this total energy is 0.18859 au. This is a correlation energy. In Hay and Dunning's calculations⁴², their correlation energy is 0.12495 au. And Meyer and Rosmus⁵¹ obtained 0.21682 au. This comparison shows that our second order H^p calculates the correlation energy reasonably well.

The total energies at various internuclear distances and separate atom limits are listed in Table 2 for NH and Table 3 for NH⁺. These values are obtained from one set of H^p matrix elements at each internuclear distances. The total energy for $X^3\Sigma^-$ state of the NH ($E = -55.15654$ au at $R = 1.985$ au) is lower than that of Neisius and Verhaegen⁴² ($E = -54.9993$ au at $R = 1.988$ au), but higher than that of Bauschlicher and Langhoff⁵⁰ ($E = -55.15754$ au at $R = 1.95$ au) who used a large basis set including $N(2f1g)$ and $H(2d)$. Bender and Davidson³⁷ obtained a little lower total energy ($E =$

Table 4. Spectroscopic Constants for the Lowest Few States of NH

		$R_e(\text{au})$	$\omega_e(\text{cm}^{-1})$	$\omega_e X_e(\text{cm}^{-1})$	$B_e(\text{cm}^{-1})$	$\alpha_e(\text{cm}^{-1})$	$D_e(\text{eV})$	$T_e(\text{eV})$
$X^3\Sigma^-$	H ^v	1.985	3267	64.7	16.24	0.56	3.54	
	POL-CI ^a	1.954	3342.6	72.9	16.76	0.616	3.27	
	CEPA ^a	1.9634	3269.3	78.8	16.60	0.648	3.38	
	CI ^b	1.97	3266	82.1	16.40	0.669	3.35	
	POL-CI ^c	2.0333	3047	86			2.83	
	GVB(1 + 2) ^f	2.005	3210	92			3.08	
	CI ^d	2.116	3224	117.2	14.28	0.564	2.62	
	MRSD + CI ^e	1.963	3264				3.495	
	MRSDCI + Q ^e	1.964	3261				3.547	
	exptl ^f	1.96	3281	77.4	16.674	0.650	3.40 ± 0.16	
$a^1\Delta$	H ^v	1.982	3295	57.7	16.29	0.54	4.35	1.820
	POL-CI ^c	2.022	3140	84			3.79	1.94
	GVB(1 + 2) ^f	1.997	3290	89			3.96	1.83
	CI ^d	2.135	3557	131.5	14.16	0.563	4.01	
	exptl ^g	1.954	3314	63			4.21	1.57
	exptl ⁱ	1.97	3186	63	16.45	0.17		
$b^1\Sigma^+$	H ^v	1.975	3347	59.2	16.41	0.54	4.47	3.038
	POL-CI ^c	2.014	3205	83			3.97	3.24
	GVB-CI ^c	2.007	3186	94			3.54	2.94
	CI ^d	2.116	3628	125.6	14.31	0.538	4.28	2.69
	exptl ^g	1.956	3355	74.4	16.401		4.34	2.64
	exptl ⁱ	1.975	3480					
$A^3\Pi$	H ^v	1.968	3271	88.4	16.54	0.69	2.17	4.001
	CI ^b	1.998	3213	127.7	16.08	0.774	1.19	
	POL-CI ^c	1.997	3180	115			1.57	4.17
	GVB-CI ^c	1.984	3225	130			1.19	4.33
	CI ^d	2.003	2941	157.1	15.87	0.874	1.38	
	exptl ^g	1.958	3188	87.5	16.69	0.744		3.70
	exptl ^h	1.959	3231	98.95	16.692	0.750	2.08	3.69
$c^1\Pi$	H ^v	2.101	2434	148.7	14.49	1.06	0.34	5.911
	POL-CI ^c	2.198	1932	330			0.12	6.06
	GVB-CI ^c	2.243	1544	598			-0.72	6.24
	CI ^d	2.21	2126	261.9	12.99	1.238	0.18	
	exptl ^g	2.081	2503	194			0.35	5.43
	exptl ⁱ	2.08	2119	190	14.165	1.267		

^aRef. 51. ^bRef. 49. ^cRef. 42. ^dRef. 38. ^eRef. 50. ^fRef. 33. ^gRef. 40. ^hRef. 34. ⁱValues Cited in Ref. 38.

-55.1620 au at $R = 1.9614$ au) than ours for this state, since they used a large basis set in their CI calculations. The total energy for $X^2\Pi$ of NH^+ ($E = -54.67011$ au at $R = 1.987$ au) is lower than that of Rosmus and Meyer⁴⁴ ($E = -54.64735$ au at $R = 2.024$ au), although they used a large basis set including $N(4f)$ and $H(3d)$.

The potential energy curves for NH and NH^+ are presented in Figure 1 and 2, respectively. To avoid complexity, the molecular states dissociating into the three or four lowest separate atom limits are shown in the Figures. As shown in Figure 1 for NH, five states are found to be bound, which corresponds very well with spectroscopy results. Hay and Dunning⁴² reported polarization CI (POL-CI) potential curves for these five bound states. And our curves are very similar to them. The first $^5\Sigma^-$ state emanating from the lowest $N(^4S^o) + H(^2S)$ separate atom limit is repulsive.

Kouba and Öhrn³⁸ showed where it crosses the $b^1\Sigma^+$ state, and Goldfield and Kirby⁴⁹ showed where it crosses the $A^3\Pi$ state. In Figure 1, the $^5\Sigma^-$ state potential curve is drawn together with other various valence state curves so that the crossing of the $^5\Sigma^-$ state with all valence states are clearly noted. The $c^1\Pi$ state has a small barrier around $R = 3.0$ au. This barrier is also noted in other CI calculations. This barrier is due to the avoided crossing between two $^1\Pi$ states coming out from two separate atom limits, i.e., $N(^2P^o) + H(^2S)$ and $N(^2P^o) + H(^2S)$. Also note in Figure 1 that the $^1\Pi$ state which has an avoided crossing with $c^1\Pi$ state is slightly bound. In Kouba and Öhrn's³⁸ CI calculations, they claim that there is the second $^2^3\Pi$ state which is bound due to avoided crossing with the $A^3\Pi$ state. But Goldfield and Kirby⁴⁹ found that the $^2^3\Pi$ state is repulsive. In our H^r calculations the second $^2^3\Pi$ state is purely repulsive. In our H^r

Table 5. Spectroscopic Constants for the Lowest Few States of NH

		$R_e(\text{au})$	$\omega_e(\text{cm}^{-1})$	$\omega_e X_e(\text{cm}^{-1})$	$B_e(\text{cm}^{-1})$	$\alpha_e(\text{cm}^{-1})$	$D_e(\text{eV})$	$T_e(\text{eV})$
$X^2\Pi$	H ^v	1.987	3426	84.8	16.31	0.59	4.37	
	CI ^a	2.022	3114	102.5	15.65	0.710	4.06	
	PNO-CI ^b	2.018	3100.1	80.7	15.71	0.606		
	CEPA ^b	2.024	3058.7	82.8	15.61	0.624	4.44	
	MO-SCF ^c	1.979	3143					
	exptl ^d		3038	58	15.67	0.64		
	exptl ^e	2.022	2922		15.35	0.64		
	exptl ^f	2.043						
$a^4\Sigma^-$	exptl ^g	2.0205			15.5891			
	H ^v	2.000	3117	138.1	16.01	0.90	3.89	0.023
	MO-SCF ^c	2.039	2865					0.06
	exptl ^f	2.088	2520					0.044
	exptl ^g	2.088	2520					
$A^2\Sigma^-$	exptl ^h	2.0643			15.0523			
	H ^v	2.211	2021	202.1	13.11	1.40	1.349	3.017
	CI ^a	2.40	1647.4	109.6	11.10	0.868	1.31	2.743
	MO-SCF ^c	2.311	1833					2.78
	exptl ^c	2.364	1585.5	61	11.455	0.6897		2.674
	exptl ^f	2.364	1707					2.67
$B^2\Delta$	H ^v	2.078	2652	111.1	14.84	0.89	3.064	3.109
	CI ^a	2.137	2409.8	134.7	14.01	0.982	3.14	3.052
	MO-SCF ^c	2.122	2477					2.90
	exptl ^d		2371	74	13.8	0.64		
	exptl ^e	2.177	2280		13.516			
	exptl ^f	2.177						2.85
$C^2\Sigma^+$	H ^v	2.098	2539	131.6	14.54	0.99	1.77	4.830
	CI ^a	2.192	2218	120.0	13.32	0.819	1.71	4.506
	MO-SCF ^c	2.15	2420					4.26
	exptl ^e	2.197	2150.5	73.0	13.265	0.789		4.285
	exptl ^f	2.230	2004					4.29

^aRef. 51. ^bRef. 49. ^cRef. 42. ^dRef. 38. ^eRef. 50. ^fRef. 33. ^gRef. 40. ^hRef. 34. (Values Cited in Ref. 38.)

calculations the second $2^3\Pi$ state is purely repulsive. So we believe that there is not much configuration mixing between these two states.

The spectroscopic constants for some NH valence states are listed in Table 4. The equilibrium internuclear distances calculated by using second order H^v are found to be in reasonable agreement with experimental values. But the H^v equilibrium distances are generally larger than corresponding experimental values. This is generally true in the second order H^v calculations. We believe that the higher order corrections to H^v are responsible for this discrepancy.

Figure 2 shows potential energy curves for some low-lying valence states of ionic NH⁺. Liu and Verhaegen's SCF level potential curves look similar to ours, but their curves for excited states are substantially different from our correlated H^v curves. It indicates the importance of correlation energy in potential curves. Kusunoki *et al.*⁴⁹ reported potential energy curves only for doublet states of NH⁺. Their multi-reference single and double CI curves are in good agreement with ours. It proves that our perturbation second order H^v is, in spirit, identical with single and double CI.

The interesting state in NH⁺ is the $a^4\Sigma^-$ state. Experimentally³² at the equilibrium internuclear distance of NH⁺,

$2^1\Pi$ state is found to be the ground state and $4^1\Sigma^-$ state is the first excited state. However, in theoretical calculations no one has not yet computed the correct ordering between the $2^1\Pi$ state and $4^1\Sigma^-$ state. In terms of molecular orbitals, the important configurations describing the $2^1\Pi$ state are $1\sigma^2 2\sigma^2 3\sigma^2 1\pi^1$, $1\sigma^2 2\sigma^2 4\sigma^2 1\pi^1$ and $1\sigma^2 2\sigma^2 3\sigma^2 4\sigma^2 1\pi^1$. For the $4^1\Sigma^-$ state, one configuration, *i.e.*, $1\sigma^2 2\sigma^2 3\sigma^2 1\pi^2$ is dominant. In theoretical calculations where certain approximations are inevitable, it is very important to calculate the correlation energy for both of the two states on an equal footing. The H^v method does have this kind of advantage (called size consistency). As shown in Figure 2, our second order H^v computations adequately generate that the $2^1\Pi$ state is the ground state and the $4^1\Sigma^-$ state is the excited state. It is the first theoretical prediction, to our knowledge, of the correct energy level ordering between the two states.

Spectroscopic constants for NH⁺ listed in Table 5 are again in reasonable agreement with experimental values. Here R_e are smaller than experimental ones. This trend is opposite to that found in NH molecule. We presume that the different choice of orbital energies for NH⁺ (bare core orbital energies) from that for NH (SCF orbital energies) is responsible for this discrepancy. As mentioned in the calculations

section, the bare core orbital energies are chosen to describe the $a^4\Sigma^-$ state properly. This problem has never been encountered in previous H^p applications. The efforts to resolve this problem will be continued in the future.

The potential energy curves of NH and NH^+ have been determined using the second order effective valence shell Hamiltonian method. Since the H^p describes the motion of valence electrons only, the H^p matrix elements which correspond to parameters in semiempirical theories have been evaluated in the *ab initio* way. The three-electron matrix elements which do not exist in semiempirical theories are found to be important in evaluating accurate valence state energies. Due to the nature of H^p , single H^p calculation accurately produces the valence state energies of neutral molecule as well as those of ions. The overall structure of the calculated potential curves for various valence state of the molecule and its ions has been reproduced accurately and it is in good agreement with that of other *ab initio* calculations. It indicates that the H^p method includes the electron correlations properly. It also signifies the fact that the H^p is a good method to generate all the valence state with same chemical accuracy.

As mentioned before, the purpose of this work is to understand the *ab initio* H^p method. In this work, it has been found that as an *ab initio* method, i) the H^p is a new and good method to treat electron correlation even including core-core, core-valence electron correlation, ii) since the H^p is based on quasidegenerate many-body perturbation theory, it can describe many states simultaneously regardless of charge states, and iii) in a computational sense, the H^p does not require effort than conventional configuration interaction calculations so that this method can be applied to bigger systems without further difficulties. As a basis for semiempirical theories, iv) since the H^p formally mimics the semiempirical Hamiltonian, it produces parameters without any ambiguity, v) the nonclassical three-electron terms should exist in an exact sense, and vi) above all, the H^p opens a new way of improving semiempirical theories in a systematic way.

Finally we would like to mention how to improve the H^p calculations in the future. First, the higher order (for example, third order) H^p may be necessary when we are interested in fine structure of molecules. Second, to have more accurate calculation results we may need to adopt a larger basis set. Lastly, to understand the H^p more deeply, wider applications of H^p to various systems may be desired.

Acknowledgement. The present study was, in part, supported by the Korea Science and Engineering Foundation No. 885-0303-003-2.

References

1. K. F. Freed, in *Modern Theoretical Chemistry*, edited by G. A. Segal (Plenum, New York, 1977), Vol. 7.
2. M. G. Sheppard, K. F. Freed, M. F. Herman, and D. L. Yeager, *Chem. Phys. Lett.*, **61**, 577 (1979).
3. M. G. Sheppard and K. F. Freed, *J. Chem. Phys.*, **75**, 4507 (1981).
4. M. G. Sheppard and K. F. Freed, *Chem. Phys. Lett.*, **82**, 235 (1981).
5. K. F. Freed, *Acc. Chem. Res.*, **16**, 137 (1983).
6. H. Sun and K. F. Freed, *J. Chem. Phys.*, **88**, 2659 (1988).
7. D. L. Yeager, H. Sun, K. F. Freed, and M. F. Herman, *Chem. Phys. Lett.*, **57**, 490 (1978).
8. H. Sun, K. F. Freed, M. F. Herman, and D. L. Yeager, *J. Chem. Phys.*, **72**, 4158 (1980).
9. K. F. Freed and H. Sun, *Israel J. Chem.*, **19**, 99 (1980).
10. H. Sun, M. G. Sheppard, and K. F. Freed, *J. Chem. Phys.*, **74**, 6842 (1981).
11. H. Sun and K. F. Freed, *Chem. Phys. Lett.*, **78**, 531 (1981).
12. T. Takada and K. F. Freed, *J. Chem. Phys.*, **80**, 3253, 3696 (1984).
13. H. Sun and K. F. Freed, *J. Chem. Phys.*, **80**, 779 (1984).
14. X. C. Wang and K. F. Freed, *J. Chem. Phys.*, **86**, 2899 (1987).
15. M. G. Sheppard and K. F. Freed, *J. Chem. Phys.*, **75**, 4525 (1981).
16. T. Takada, M. G. Sheppard, and K. F. Freed, *J. Chem. Phys.*, **79**, 325 (1983).
17. Y. S. Lee and K. F. Freed, *J. Chem. Phys.*, **79**, 839 (1983).
18. Y. S. Lee, H. Sun, D. L. Yeager, and K. F. Freed, *J. Chem. Phys.*, **79**, 3862 (1983).
19. M. R. Hoffmann, X. C. Wang, and K. F. Freed, *Chem. Phys. Lett.*, **136**, 392 (1987).
20. X. C. Wang and K. F. Freed, *J. Chem. Phys.*, **91**, 3002 (1989).
21. H. Sun, K. F. Freed, and Y. S. Lee, *Chem. Phys. Lett.*, **15**, 529 (1988).
22. B. H. Brandow, *Adv. Quantum Chem.*, **10**, 188 (1977), and references therein.
23. I. Lindgren, *Rep. Prog. Phys.*, **47**, 345 (1984), and references therein.
24. R. G. Parr, *The Quantum Theory of Molecular Electronic Structure*, (Benjamin, New York, 1963).
25. M. J. S. Dewar, *The Molecular Orbital Theory of Organic Chemistry*, (McGraw-Hill, New York, 1969).
26. J. A. Pople and D. L. Beveridge, *Approximate Molecular Orbital Theory*, (McGraw-Hill, New York, 1970).
27. R. J. Celotta, R. A. Bennett, and J. L. Hall, *J. Chem. Phys.*, **60**, 1740 (1974).
28. W. H. Smith, J. Brzozowski, and P. Erman, *J. Chem. Phys.*, **64**, 4628 (1976).
29. O. Gustafsson, G. Kindvall, M. Larsson, B. J. Olsson, and P. Sigra, *Chem. Phys. Lett.*, **138**, 185 (1987).
30. R. Colin and A. E. Douglas, *Can. J. Phys.*, **64**, 61 (1968).
31. I. Kusunoki and Ch. Ottinger, *J. Chem. Phys.*, **80**, 1872 (1984).
32. K. Kawaguchi and T. Amano, *J. Chem. Phys.*, **88**, 4584 (1988).
33. H. Sakai, P. Hansen, M. Esplin, R. Jahansson, M. Petola, and J. Strong, *Appl. Opt.*, **21**, 228 (1982).
34. J. Malicet, J. Brion, and H. Guenebaut, *J. Chim. Phys.*, **67**, 25 (1970).
35. E. R. Davidson, L. E. McMurchie, S. T. Elbert, S. R. Langhoff, D. Rawlings, and D. Feller, *IMS Computer Center, Library Program No. 030*.
36. G. Herzberg and J. W. C. John, *Astrophys. J.*, **158**, 399 (1969).
37. C. F. Bender and E. R. Davidson, *Physical Rev.*, **183**, 23 (1969).
38. J. Kouba and Y. Öhrn, *J. Chem. Phys.*, **52**, 5387 (1970).
39. H. P. D. Liu and G. Verhaegen, *J. Chem. Phys.*, **53**, 735 (1970).

40. S. V. O'Neil and H. F. Schaefer, *J. Chem. Phys.*, **55**, 394 (1971).
41. J. M. Lents, *J. Quant. Spectrosc. Radiat. Transfer.*, **13**, 297 (1973).
42. P. J. Hay and T. H. Dunning, *J. Chem. Phys.*, **64**, 5077 (1976).
43. A. Banerjee and F. Grein, *J. Chem. Phys.*, **66**, 1054 (1977).
44. P. Rosmus and W. Meyer, *J. Chem. Phys.*, **66**, 13 (1977).
45. V. Klimo and J. Jino, *Mol. Phys.*, **41**, 477 (1980).
46. D. Neisius and G. Verhaegen, *Chem. Phys. Lett.*, **89**, 228 (1982).
47. S. A. Pope, I. H. Hillier, and M. F. Guest, *Faraday Symp. Chem. Soc.*, **19**, 109 (1984).
48. U. Mänz, A. Zilch, P. Rosmus, and H. J. Werner, *J. Chem. Phys.*, **84**, 5037 (1986).
49. E. M. Goldfield and K. P. Kirby, *J. Chem. Phys.*, **87**, 3986 (1987).
50. C. W. Bauschlicher and S. R. Langhoff, *Chem. Phys. Lett.*, **135**, 67 (1987).
51. W. Meyer and P. Rosmus, *J. Chem. Phys.*, **63**, 2356 (1975).
52. L. Farnell and J. F. Ogilvie, *J. Mol. Spectrosc.*, **101**, 104 (1983).
53. I. Kusunoki, K. Yamashita, and K. Morokuma, *Chem. Phys. Lett.*, **123**, 533 (1986).
54. L. Farnell and J. F. Ogilvie, *Chem. Phys. Lett.*, **137**, 191 (1987).
55. K. Yamashita, S. Yabushita, K. Morokuma, and I. Kusunoki, *Chem. Phys. Lett.*, **137**, 193 (1987).
56. T. H. Dunning, *J. Chem. Phys.*, **53**, 2823 (1970).
57. F. B. van Duijneveldt, *IBM J. Res.*, **945**, No. 16437 (1971).

Electrochemical Polymerization of Pyrrole from Aqueous Solutions: 2. Growth Kinetics of Polypyrrole *p*-toluenesulfonate Film

Eui Hwan Song and Woon-Kie Paik *

Department of Chemistry, Sogang University, Seoul 121-742

Jung-Kyoon Chon

Department of Chemistry, Hankuk University of Foreign Studies, Seoul 130-791. Received October 26, 1989

The rates of electropolymerization of pyrrole from aqueous solutions containing *p*-toluenesulfonic acid were studied as functions of the concentration of the surfactant anions and of temperature for the polymerization on the electrode surface immersed in the solution and also for the polymerization along the solution surface. In the case of the *solution-surface polymerization*, the polymerization rate showed maximum as the concentration of the *p*-toluenesulfonic acid changed at a fixed temperature or as the temperature was varied at a fixed concentration. The decrease of the polymerization rate with increasing concentration or with rising temperature beyond the values at the maxima is interpreted as resulting from micelle formation.

Introduction

In recent years, there have been numerous investigations¹⁻⁹ on the electropolymerization of pyrrole in various solvents to obtain polypyrrole which is electronically conducting when anodically "doped" with anions. Polypyrrole (PPy) films incorporated with surface-active anions have recently received considerable interest because of the enhanced mechanical and conducting properties¹⁰. In a previous communication¹¹ we reported that polymerization of pyrrole can occur not only on the surface of an electrode immersed in the solution (*in-solution polymerization*) but also along the solution surface when the electrode is placed horizontally touching on the surface of the solution (*solution-surface polymerization*). The *solution-surface polymerization* was achieved by using an aqueous pyrrole solution containing surfactant anions, such as *p*-toluenesulfonic acid (*p*-TSA) and sodium dodecylsulfate. The polymer obtained by the

solution-surface polymerization was in the form of thin film attached on both sides of the platinum wire or in the form of fibrillar bundles depending on the electrolytes used. The polypyrrole film obtained by the *solution-surface polymerization* method using *p*-toluenesulfonic acid (*p*-TSA) had improved mechanical and conducting properties in comparison with the ones obtained by the *in-solution polymerization* method, although the structural units of the conducting polymers obtained by the two methods were both approximately [(Py-Py)⁺A⁻].

In this paper, we report our results of a comparative study on the growth rate of the polypyrrole *p*-TSA films by the *in-solution polymerization* and the *solution-surface polymerization* techniques.

Experimental

Pyrrole (from Fluka) was purified by vacuum distillation